JOURNAL OF AGRICULTURAL AND FOOD CHEMISTRY

# Impact of Casein Gel Microstructure on Self-Diffusion Coefficient of Molecular Probes Measured by $^1$H PFG-NMR

STEVEN LE FEUNTEUN AND FRANÇOIS MARIETTE*

Cemagref, Process Engineering Technology Research Unit, CS 64426, 17 avenue de Cucillé, 35044 Rennes, Cedex, France

The translational dynamics of poly(ethylene glycol) (PEG) polymers with molecular weights ($M_w$) varying from $6 \times 10^2$ to $5 \times 10^5$ were investigated by pulsed field gradient NMR in casein suspensions and in gels induced by acidification, enzyme action, and a combination of both. For molecules with $M_w \leq 1020$, the diffusion was only dependent on the casein concentration whatever the molecular weight of the probe or the sample studied. However, for PEG with $M_w \geq 8000$, there was strong dependence of diffusion on PEG size and on the casein network structure as revealed by scanning electron microscopy images. The diffusion coefficients of the two largest PEGs were increased after coagulation by amounts that depended on the internal structure of the gel. In addition, the 527 000 g/mol PEG was found to deviate from Gaussian diffusion behavior to greater or lesser extents according to the casein concentration and the sample microstructure. The results are discussed in terms of network rearrangements.

**KEYWORDS: Diffusion; NMR; stretching exponent; curved echo decay; PEG; PEO; probe; tracer; casein; micelle; gel; acid; chymosin; rennet; structure**

## INTRODUCTION

Caseins are the major proteins of milk, and they are directly involved in the formation of dairy gels because they constitute the building blocks of the network. Classical processes involving acid and rennet coagulation or combinations of both are used to convert milk into gels such as yogurt or cheese curd. Acid gels are obtained through the acidification of the medium, and rennet gels are formed by enzymatic hydrolysis (by chymosin). It is well-known that these different types of gel do not have the same rheological and structural properties. For example, rennet gels are more viscous than their acid counterparts, and gels made by the concomitant action of an enzyme and an acid are constituted of thicker aggregates and larger pores (*1*). Functional properties such as water holding capacity or permeability are therefore different within rennet and acid gels (*2, 3*). However, very little is currently known about the impact of these different types of coagulation on diffusion processes.

In this study, the self-diffusion of probes was investigated in various casein matrices. Diffusion measurements were carried out with the Pulsed Field Gradient NMR (PFG-NMR) technique because this method has been proven to be very powerful in applications dealing with progressively more "difficult" samples, including systems that involve compositional complexity or morphological heterogeneity. The probe molecules used are poly(ethylene glycol) (PEG) and poly(ethylene oxide) (PEO) for low and high molecular weights, respectively (both types of polymer will be referred to PEG as they differ by only one chain end). Numerous PFG-NMR studies have been performed on PEG self-diffusion in various matrices such as polymer solutions and gels (*4–17*), whey protein systems (*18*), cartilage (*19*), wet cotton (*20*), agarose gels (*21*), and alginate samples (*22, 23*). One of the main conclusions arising from these studies is that the sample structure has an influence on PEG diffusion. For a given molecular weight and a given matrix concentration, normalized self-diffusion coefficients can be very different according to the microstructure of the matrix.

Studies have also been carried out on the self-diffusion of water (*24–26*) and PEGs (*27*) in casein suspensions and in rennet gels. According to Mariette et al. (*26*), water diffusion in casein systems can be explained by two diffusion pathways, one around and the other through the casein micelles. The obstruction effect on water diffusion was akin to local restrictions at the casein surface and explained the absence of an effect of casein gelation by rennet. A more complex behavior was observed for PEG molecules. First, the diffusion coefficients were dependent on both the casein concentration and on the PEG size; the larger the PEG size, the greater the hindrance to diffusion. Second, the formation of a rennet gel resulted in an enhanced diffusion coefficient for large probes. As for water, the model with two compartments was used to describe the results in solutions and gels. According to this model, the increase in the diffusion coefficients could be explained by a decrease in the casein

* Corresponding author. Telephone: 33 (0)223482121, fax: 33(0)223482115, e-mail address: Francois.Mariette@cemagref.fr.

10.1021/jf071982v CCC: $37.00 
Published on Web 11/30/2007

**Table 1.** Composition of Micellar Casein Powder

| | micellar casein powder (%) |
|---|---|
| total solids (g/kg) | 100 |
| total nitrogen matter (g/kg) | 90.7 |
| noncasein nitrogen (g/kg) | 5.7 |
| nonprotein nitrogen (g/kg) | 0.6 |
| calcium (g/kg) | 2.9 |
| ash (g/kg) | 8.1 |
| pure caseins (g/kg) | 85.0 |

hydration, and hence by a change in the sample microstructure. However, the model failed to describe the diffusion of the largest PEG studied (634 000 g/mol). Moreover, this PEG was the only one where a curvature was observed in the echo decays of the diffusion spectra despite its low polydispersity index. More information is required regarding these phenomena to provide greater understanding of the mechanisms that influence molecular diffusion.

In the present study, changes in the diffusion rate of PEGs within casein suspensions and acid gels of different casein concentrations were compared. PEG self-diffusion measurements are also reported for three different types of casein networks formed from concentrated casein solutions. These diffusion findings were compared to SEM images to improve the understanding of the influence of the microstructure on solute diffusion. In addition, we discuss various reasons for the presence of an anomalous diffusion behavior observed for the largest polymer. We demonstrate that all the results presented can be explained qualitatively with a single interpretation based on network rearrangements. This study is an extension of previously published work (*18*, *27*).

## MATERIALS AND METHODS

**Materials.** Native phosphocaseinate powder (INRA, Rennes, France) was used (**Table 1**). PEGs with different $M_w$ values (620, 1020, 8440, 96 750, and 527 000) and low polydispersity indices ($M_w/M_n = 1.06$, 1.04, 1.05, 1.06, and 1.06, respectively) were obtained from Polymer Laboratories (Marseilles, France). Sodium azide (Merck, Darmstadt, Germany), sodium chloride, and glucono-$\delta$-lactone (GDL), with a purity above 99% (Sigma-Aldrich, Steinheim, Germany), were used without purification. $D_2O$ (purity >99.8%) was purchased from Cortecnet (Paris, France), and the chymosin solution used was Chymax-Plus (Chr Hansen, Arpajon, France).

**Preparation of Native Phosphocaseinate Suspension (NPCS).** Rehydration of the powder was performed at room temperature over 36 h with $D_2O$ containing 0.1 M NaCl and 0.2% (w/w) $NaN_3$ to prevent bacterial growth. Once the powder was totally rehydrated, 0.1% (w/w) of PEG was added to the casein suspensions regardless of molecular weights. The pD measured was 6.80 in all samples.

**Determination of Dry Matter.** The dry matter of all casein suspensions was verified by measuring variations in weight after drying in an oven for 24 h at 100 °C. Concentrations were then calculated from the pure casein percentage (**Table 1**) and ranged from 4.8 to 15.0 g of casein for 100 g of $D_2O$.

**Acid Gels.** According to the casein concentration, defined amounts of GDL were added to solutions to reach a final pD of 4.60 ± 0.05. After addition of GDL, casein suspensions were stirred for 5 min, and small amounts of the suspension were transferred to 5 mm NMR tubes (~1 mL) that were kept at room temperature for 48 h before analysis. No shrinkage occurred within this interval.

**Enzymatic Gels.** A chymosin dilution (1 mL in 99.0 g of distilled water) was always prepared 20 min before each inoculation. All enzymatic gels had a casein concentration of 15.0 g/100 g $D_2O$ and were induced by addition of 336 $\mu$L of the chymosin dilution to 10 g of NPCS. The samples were then stirred for 5 min, and small amounts were transferred to 5 mm NMR tubes. NMR tubes were then placed in a water bath for 2 h at 30 °C, after which they were cooled to room temperature. Analyses were carried out 24 h after inoculation. No shrinkage occurred within this interval.

**Combined Gels.** The casein concentration used was 15.0 g/100 g $D_2O$. The same procedure as for enzymatic gels was used to form combined gels, except that 410 mg of GDL was added to the 10 g of NPCS at the same time as the chymosin. The final pD was 4.60 ± 0.05 in all samples. Combined gels were analyzed 24 h after inoculation. No shrinkage occurred within this interval.

**pD Measurement.** All pD values were calculated from the equation: $pD = pH_{nom} + 0.40$ (*28*), where $pH_{nom}$ is the nominal reading of our pH-meter (Schott, combination electrode type no. N6280, Germany).

**Scanning Electron Microscopy (SEM).** Small cubes of the gels (5 × 5 × 5 mm) were immersed in 2.5% v/v glutaraldehyde at 20 °C for 48 h in a sodium cacodylate buffer, pH 7.2. Samples were rinsed several times with distilled water before being dehydrated in a graded ethanol series (10–30–50–70–80–90–95–100% (v/v)) in 20 min steps and finally conserved in acetone (purity >99.9%) for one night. Samples were then dried using $CO_2$ in a critical-point drier (CPD 010, Balzers Union Ltd., Liechtenstein). Dried samples were fractured, mounted onto specimen stubs, gold coated, and analyzed microscopically using a scanning electron microscope (Jeol JSM 6301F) operated at an acceleration voltage of 9 kV. The images were produced by Centre de Microscopie Électronique à Balayage et microAnalyse (CMEBA, France, Rennes).

**NMR Self-Diffusion Measurements.** All measurements were performed at 20 ± 0.1 °C on a 500 MHz Bruker spectrometer equipped with a field gradient probe. The BPP-LED sequence (*29–31*) was used with 16 different gradient strengths ($g$) ranging from ~0.25 to 6.00 T/m and a gradient length ($\delta$) equal to 1.0 ms. The diffusion interval ($\Delta$) was adjusted to maintain a constant diffusion distance $z \sim 1.5\ \mu$m, in accordance with the Einstein equation $z = (2D\Delta)^{1/2}$. Sixteen scans were carried out, and the recycle delay was set at $5T_1$.

**Theoretical Considerations and Processing Methods.** All data processing was performed with Matlab software, and all fits were performed by nonlinear least-squares methods. Monte-Carlo simulations were used for error calculations with 200 iterations. In a PFG-NMR experiment using the BPP-LED sequence, the echo intensity ($I$) is described by the following equation,

$$I/I_0 = \sum_i p_i \exp(-kD_i) \tag{1}$$

with

$$k = \gamma^2 g^2 \delta^2 \left(\Delta - \frac{\delta}{3} - \frac{\tau}{2}\right) \tag{2}$$

where $I_0$ is the signal intensity in the absence of gradients, $\gamma$ is the gyromagnetic ratio (for protons, $\gamma = 26.7520 \times 10^7$ rad T$^{-1}$ s$^{-1}$), $g$ is the amplitude of the gradient pulse, $\delta$ is the gradient pulse duration, $\Delta$ is the time between the leading edges of gradient pulses, $\tau$ is the time between the end of each gradient and the next radiofrequency pulse, $D_i$ is the self-diffusion coefficient of the $i$th component, $p_i$ is the fractional proton number of the $i$th component, and $\Sigma p_i = 1$ (in this study, $i = 1$ or 2).

Eq. 1 was used for HOD (monodeuterated water) and PEGs with $M_w < 527\,000$. For the largest PEG, an increasing nonexponential trend was observed as the concentration increased. It was found that a stretched exponential of the following form constituted a very good approximation for the decay function at all concentrations (eq 3).

$$I/I_0 = \exp[-(kD_{app})^{\beta}] \tag{3}$$

Here, $D_{app}$ is an apparent diffusion coefficient, and $\beta$ is the "stretching exponent". This approach has been used in a number of previous studies (*23*, *32–36*). The $\beta$ parameter describes the width of the distribution of diffusion coefficients. $\beta$ is equal to one for a monodisperse system and decreases from unity if the width of the diffusion

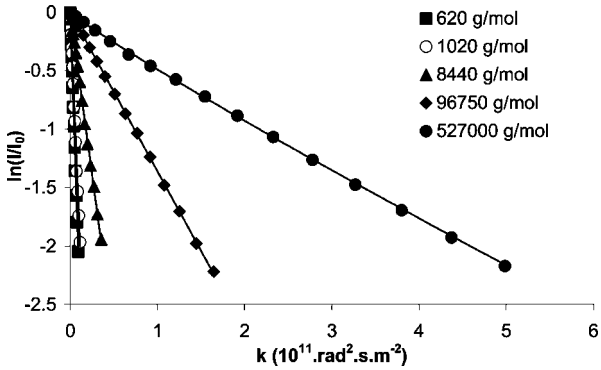


**Figure 1.** Stejskal−Tanner plots of PEGs in a $D_2O$/NaCl solution (0.1 M) at 20 °C for different PEG molecular weights. Solid lines are linear regressions except for the 527 000 g/mol PEG, where the line is the fit curve obtained with the stretched exponential approach (eq 3).

coefficient distribution becomes greater. A mean self-diffusion coefficient $D_{mean}$ can be obtained through eq 4,

$$D_{mean} = \frac{D_{app}}{\frac{1}{\beta}\Gamma\left(\frac{1}{\beta}\right)} \quad (4)$$

where $\Gamma$ is the gamma function.

*In NPCS and in Enzymatic Gels*, all diffusion coefficients were obtained by fitting eq 1, with $i = 1$, to the raw NMR data. In an ordinary $^1$H NMR spectrum, the PEG peak overlaps with casein signals at ~3.6 ppm. However, because of the very short relaxation times ($T_1$, $T_2$) of casein protons, their signals were severely attenuated in BPP-LED spectra and did not contribute to PEG echo intensity.

*In Acid and Combined Gels*, water diffusion was obtained as before by eq 1, but in these samples PEGs and gluconic acid, which is formed by hydrolysis of GDL, presented an overlapping signal in the diffusion spectra. For such NMR data, the diffusion coefficients of each component can be calculated by fitting eq 1 with $i = 2$. This method was used for the 96 750 g/mol and 8440 g/mol PEGs. However, because smaller PEGs (620 and 1020 g/mol) and gluconic acid have very similar diffusion coefficients, the latter method appeared inefficient for separation of each component. For such samples, the diffusion coefficient of gluconic acid was first determined from an isolated and specific peak of the latter. The proportion of the gluconic acid signal overlapping with the PEG signal was then estimated by taking an isolated casein signal as reference. These two values were finally reintroduced in eq 1 with $i = 2$ to estimate the diffusion coefficients of the 620 and 1020 g/mol PEGs in acid and combined gels. For the 527 000 g/mol PEG, the gluconic acid signal was totally attenuated in the third spectrum of the diffusion spectra. Results for this polymer were thus obtained by fitting eqs 3 and 4 to the NMR data, after eliminating the first two intensities. In the rest of this paper, all diffusion data presented for the 527 000 g/mol PEG are $D_{mean}$ values.

## RESULTS

**PEG Self-Diffusion in $D_2O$.** Stejskal−Tanner plots obtained at 20 °C for each PEG in a $D_2O$/NaCl solution (0.1 M) are given in **Figure 1**. Except for the largest PEG, all echo attenuations were linear, indicating that there was no need to account for mass polydispersity effects. For the 527 000 g/mol PEG, in which a slight curvature was found, the stretched exponential approach was used to account for the distribution of diffusion coefficients. The $\beta$ value obtained was 0.92, which indicates the presence of a polydispersity effect for this polymer. The molecular weight, polydispersity index, and self-diffusion coefficient measured for all polymers studied are summarized in **Table 2**. All of these findings are in accordance with previous studies (*4, 6, 27*).

**Table 2.** Self-Diffusion Coefficients of the PEGs Studied in a $D_2O$/NaCl Solution (0.1 M) at 20 °C

| $M_w$ | $M_w/M_n$ | D $m^2$ $s^{-1}$ |
|---|---|---|
| 620 | 1.06 | $2.26 \times 10^{-10}$ |
| 1020 | 1.04 | $1.81 \times 10^{-10}$ |
| 8440 | 1.05 | $5.59 \times 10^{-11}$ |
| 96 750 | 1.06 | $1.37 \times 10^{-11}$ |
| 527 000 | 1.06 | $4.67 \times 10^{-12}$ |

**Normalization of Coefficients Diffusion.** The self-diffusion coefficients presented in **Table 2** cannot be directly used to normalize the diffusion coefficients obtained in casein suspensions and gels. Gluconic acid (when present) and soluble residues of the protein powder contribute to molecular diffusion hindrance in the aqueous phase. To consider the effects of casein alone, it is necessary to normalize the self-diffusion coefficient in casein samples ($D$) by $D_0$, the self-diffusion coefficient in the water phase, including these soluble compounds (*25*).

The effects of the soluble powder residues on polymer diffusion were calculated according to the approach described by Colsenet et al. (*27*). This method enabled us to compare diffusion coefficients in solutions and in enzymatic gels but not those measured in acid or combined gels because the hindrance caused by the addition of GDL must also be considered. Diffusion measurements were thus performed for each PEG in $D_2O$ with different amounts of GDL. The results are illustrated in **Figure 2**. They revealed that the reduction in diffusion was exactly the same whatever the PEG molecular weight. The effect of the addition of GDL was thus explained simply by an increase in bulk viscosity, and a general linear regression was therefore performed on all data. Consequently, in acid and combined gels, once the effect of the powder soluble residues had been taken into account, the self-diffusion coefficients in the aqueous phase ($D_0$) were predicted from this equation. All of the data discussed in this paper are thus reduced self-diffusion coefficients defined as $D_R = D/D_0$, where $D$ is the self-diffusion coefficient measured in the sample.

**pD effect.** Diffusion coefficients of the 96 750 g/mol PEG were measured in $D_2O$ for different pD values to check for a possible effect of acidity on polymer diffusion. Final pD values were obtained by adding a few drops of a HCl/$D_2O$ dilution in 10 g $D_2O$ containing 0.1% (w/w) PEG. As illustrated in **Figure 3**, the results showed that the acidity of $D_2O$ solutions had no effect on PEG diffusion.

**PEG Self-Diffusion Coefficients in Casein Suspensions.** Self-diffusion coefficients of PEGs in various solutions were measured at 20 °C for different casein concentrations. Stejskal−

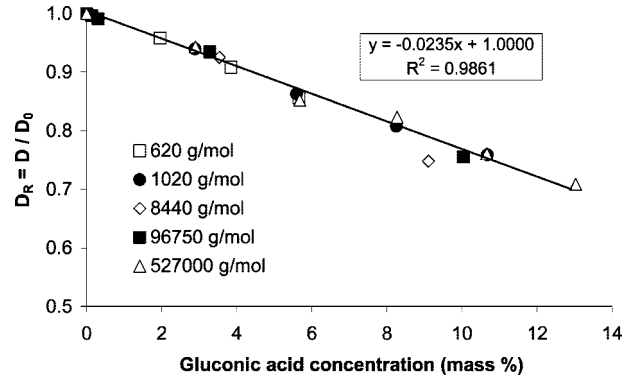


**Figure 2.** Dry matter effect of gluconic acid on reduced PEG self-diffusion coefficients measured at 20 °C. The solid line is the linear regression of the data.

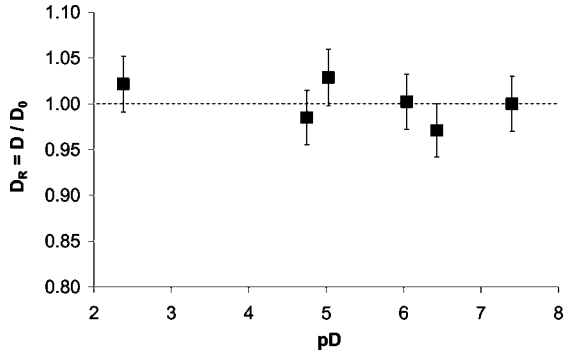


**Figure 3.** Reduced self-diffusion coefficients of the 96 750 g/mol PEG at 20 °C at different pD values in $D_2O$ solutions. Error bars are 5%.

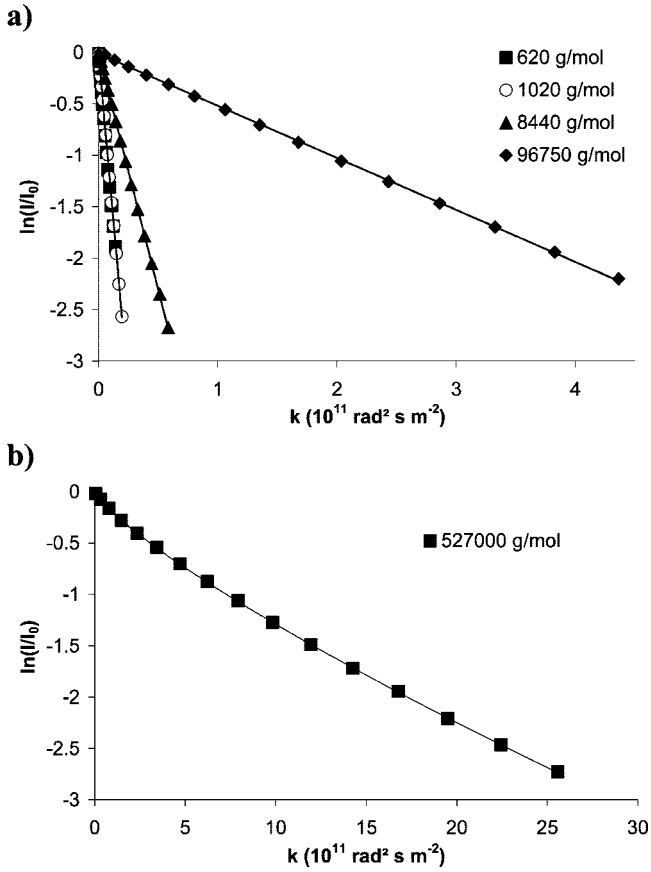


**Figure 4.** Stejskal−Tanner plots of PEGs in a casein suspension (15 g/100 g $D_2O$) at 20 °C: (**a**) 620, 1020, 8440, and 96 750 g/mol PEGs, solid lines are linear regressions; (**b**) 527 000 g/mol PEG, the solid line is the fit curve obtained with the stretched exponential approach (eq 3).

Tanner plots obtained for all PEGs at a high casein concentration are given as an example in **Figure 4**. As observed in $D_2O$, a linear decrease in the echo intensities was found for all polymers, except for the largest PEG. However, for the latter polymer, the curvature was clearly enhanced in the concentrated casein suspension (**Figure 1** and **Figure 4b**). To illustrate this phenomenon, the widths of the diffusion coefficient distributions ($\beta$) obtained in NPCS are illustrated in **Figure 5** as a function of casein concentration. The $\beta$ value remained constant below approximately 9 g/100 g $D_2O$, but for more concentrated solutions there was an increase in the width of the distribution ($\beta$ decreased), suggesting a change in the diffusion mechanism above this concentration.

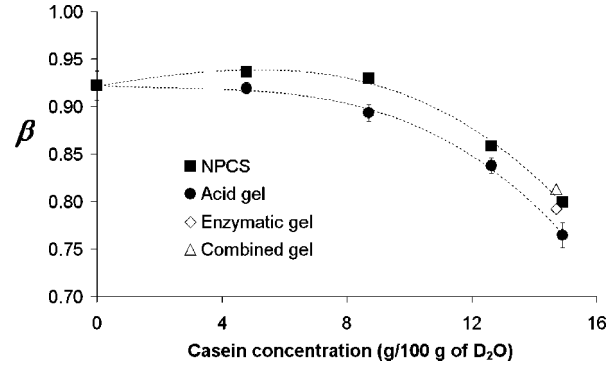


**Figure 5.** The width of the self-diffusion coefficient distribution of the 527 000 g/mol PEG ($\beta$) as a function of casein concentration in NPCS and acid gels. The $\beta$ values obtained in the enzymatic and combined gels are also presented. Dotted lines are guides for the eyes.

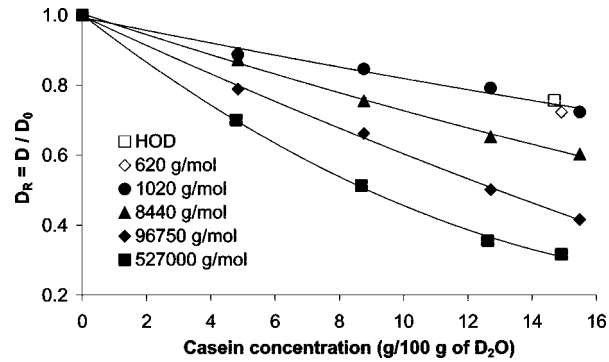


**Figure 6.** Reduced self-diffusion coefficients of water and the different PEGs as a function of casein concentration in casein suspensions. Solid lines are guides for the eyes.

**Figure 6** illustrates the calculated $D_R$ values of water and PEGs plotted as a function of casein concentration in NPCS. $D_R$ decreased when more casein was added for all the systems studied. The diffusion of water and of the two smallest PEGs (620 and 1020 g/mol) was identically hindered in the presence of casein micelles, but for the other polymers the reduction in the diffusion rate was sensitive to PEG size. These results are in complete agreement with the results obtained in casein suspensions by Colsenet et al. (*27*). Nevertheless, we demonstrated that the same hindrance to diffusion occurred below a molecular weight around 1020, suggesting a similar mechanism of obstruction by casein micelles.

**Acid Gelation Effect.** Diffusion measurements of the 96 750 g/mol PEG in a concentrated acid gel (15.0 g/100 g $D_2O$) were carried out for different distances probed. The Stejskal−Tanner plots are given in **Figure 7** for $\Delta$ values of 14.3, 25, 100, 200, and 1000 ms. The results demonstrated that the PEG self-diffusion coefficient was the same whatever the distance traveled between 0.4 and 3.4 $\mu$m. This indicates that no restricted diffusion occurred and that the gel appeared homogeneous on the length-scale studied (1.5 $\mu$m). However, caution must be applied when trying to extrapolate these findings to the largest polymer because of its anomalous diffusion behavior (**Figure 4b**).

**Figure 8** shows the reduced PEG self-diffusion coefficients in acid gels divided by those in solutions ($D_R^{gel}/D_R^{sol}$) plotted as a function of casein concentration. This ratio is very convenient for visualizing the effect of the microstructure alone. $D_R^{gel}/D_R^{sol}$ was equal to one for the three smallest PEGs (620, 1020, and 8440 g/mol) whatever the casein concentration, and hence the acid coagulation had no influence on the diffusion of

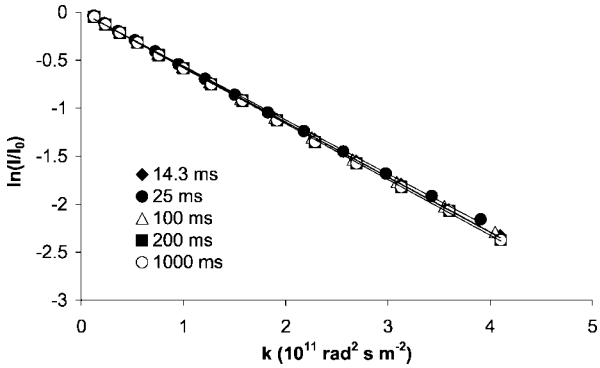


**Figure 7.** Stejskal−Tanner plots of 96 750 g/mol PEG in an acid casein gel (15.0 g/100 g $D_2O$) for different diffusion intervals ($\Delta$) at 20 °C. Solid lines are linear regressions.

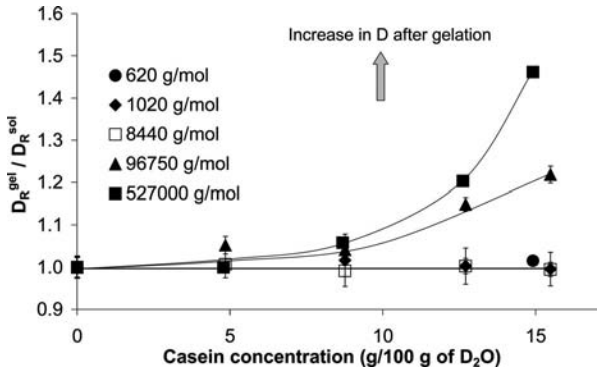


**Figure 8.** $D_R^{gel}/D_R^{sol}$ ratios obtained for all PEGs as a function of casein concentration for different PEG molecular weights at 20 °C. Solid lines are guides for the eyes.

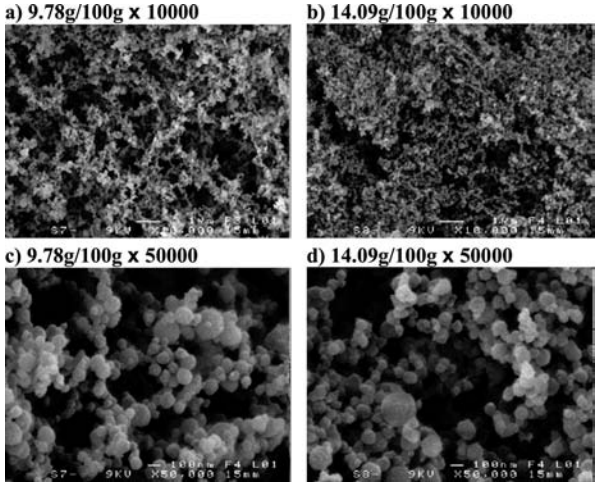


**Figure 9.** SEM images of acid casein gels at two magnifications and two casein concentrations: 9.78 g/100 g $D_2O$ (panels **a** and **c**) and 14.09 g/100 g $D_2O$ (panels **b** and **d**).

these polymers. However, for the two largest PEGs (96 750 and 527 000 g/mol), diffusion was faster in gels than in the liquid state, and this effect increased with both the casein concentration and PEG size. In parallel, the stretched parameter $\beta$ for the 527 000 g/mol PEG was always reduced in the gel system, indicating that the width of the distribution of diffusion coefficients was enlarged (**Figure 5**).

SEM pictures of acid gels at two different concentrations are presented in **Figure 9**. The images show coarse networks constituted of small casein aggregates linked together. The gel structures appeared homogeneous on a scale of few micrometers,

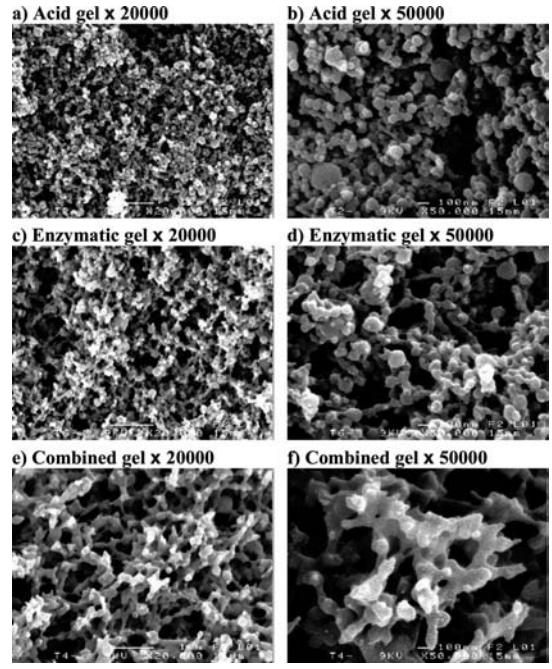


**Figure 10.** SEM images of an acid gel (panels **a** and **b**), an enzymatic gel (panels **c** and **d**), and a combined gel (panels **e** and **f**) at two magnifications. All gels were formed from the same concentrated casein solution (15.0 g/100 g $D_2O$).

which is consistent with the constant value of the diffusion coefficient of the 96 750 g/mol PEG obtained for different diffusion intervals ($\Delta$, **Figure 7**). As can be seen at higher magnifications (**Figure 9**, panels **c** and **d**), the gel was formed of aggregated spherical particles with a mean diameter of approximately 150 nm. The same network organization and microstructure were observed for all concentrations. The decrease in PEG diffusion when the casein concentration increased could therefore be attributed to a simple obstruction effect.

**Comparison of Effects of Enzymatic, Acid, and Combined Gelation.** The SEM images of the three gels studied (15 g/100 g $D_2O$) illustrated in **Figure 10** show that all the microstructures appeared homogeneous at a scale of several micrometers. As reported above, the acid gel was composed of small spherical particles and pores (**Figure 10**, panels **a** and **b**). The combined gel presented a different network organization (**Figure 10**, panels **e** and **f**). Its microstructure appeared more branched and was formed of highly fused casein aggregates that formed thick strands leaving large pores in between. An intermediate structure was observed in the enzymatic gel (**Figure 10**, panels **c** and **d**). As in the acid gel, small spherical particles were present, but at the same time there were stretched strands and larger pores.

Self-diffusion coefficients measured in each type of gel are presented in **Figure 11** for all the molecules studied. The $D_R^{gel}/D_R^{sol}$ ratio for water and small PEGs (620, 1020, and 8440 g/mol) were always equal to one, but the diffusion was faster in gels for the two largest PEGs. This effect was strongly dependent on gel type, because the increase in the diffusion rate of both PEGs was greater in the combined gel, followed by the enzymatic gel, and finally the acid gel. In parallel, the $\beta$ values obtained for the 527 000 g/mol PEG in the different gels are illustrated in **Figure 5**. As explained above, reduction of $\beta$ was observed after acid gelation. This decrease in $\beta$ was smaller for the enzymatic gel, and for the combined gel a slight increase in $\beta$ was observed. It thus appeared that the diffusion coefficients

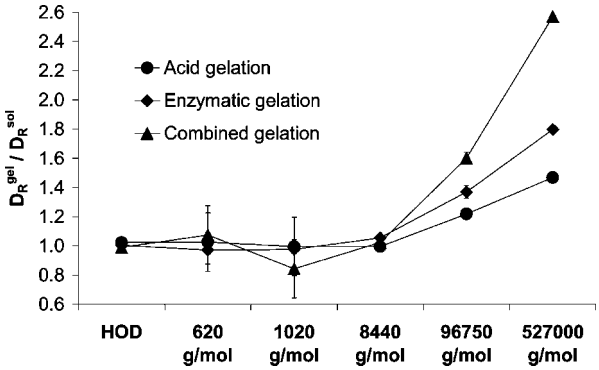


**Figure 11.** $D_R^{gel}/D_R^{sol}$ ratios obtained at 20 °C for HOD and all PEGs in concentrated enzymatic, acid, and combined gels (15.0 g/100 g $D_2O$). Solid lines are guides for the eyes, and error bars were arbitrarily set at 20% for the 620 and 1020 g/mol PEGs in acid and combined gels because of the processing method employed.

and the $\beta$ values varied in the gel state, together with the gel microstructures, indicating that all these findings are probably interlinked.

## DISCUSSION

Caseins are present in milk in the form of a suspension of spherical particles called casein micelles. These colloidal particles contain many thousands of individual casein molecules. The overall diameter of micelles ranges from 50 to 500 nm, with a mean diameter around 150 nm (*37*). Numerous models of the internal structure of the casein micelle have been proposed, and it now seems that caseins are held together by hydrophobic and electrostatic interactions and that nanoclusters are formed around the colloidal calcium phosphate (*38–41*). All authors agree that micelle stability is provided by a surface layer of $\kappa$-casein, which confers steric and electrostatic stabilization on the particles (*42, 43*). They are known to be very porous, and hydration values reported in the literature are generally around 3 or 4 g of water per 1 g of casein (*44–48*).

Casein gels are usually classified as particle gels, although it is now realized that they differ in important aspects from gels formed of hard particles (*41, 49*). They are generally subdivided according to the way in which they are formed, that is, by enzyme action, acidification, or a combination of both. Acidification of milk reduces the negative charges of $\kappa$-caseins on the micelle surface and results in the coagulation of the system. All the calcium phosphate contained by micelles is progressively dissolved in the aqueous phase, and the final gel firmness is low. In comparison, enzymatic gels are formed by the addition of an enzyme that hydrolyses the C-terminal part of the $\kappa$-caseins, thereby reducing steric and electrostatic stabilization of the casein micelles and causing them to aggregate. The mineral balance between the aqueous and colloidal phases remains constant, and the final gels generally present much greater firmness and often exhibit syneresis.

In all casein gels, structural changes take place during aging and are generally explained in terms of rearrangements of the gel network. They constitute an important phenomenon because they cause changes in the gel microstructure and rheological characteristics. For instance, Lucey et al. (*50*) reported that, in acid gels, considerable rearrangement of particles in the network is associated with high permeability. In rennet gels, Bauer et al. (*51*) described that "increasingly compact objects" were formed after the aggregation process. Indeed, comparisons between casein gel microstructures and properties are often discussed in terms of variations in the extent of rearrangements (*1–3, 52–55*). In a comprehensive review, Mellema et al. (*49*) proposed a model based on four structural levels to describe casein particle rearrangements. The phenomena are not fully understood, but all authors agree on the fact that they give rise to aggregate fusion, local matrix compaction, and the formation of larger gel pores. It follows that the structural rearrangements that take place after the aggregation stage result in a decrease in the volume occupied by the casein aggregates. As discussed below, our findings are very consistent with this understanding of the formation of dairy gels, and can be broken down according to the size of the diffusing molecule.

**Diffusion of Molecules with $M_w \leq 1020$.** The results presented in **Figure 6** are in very good accord with previous findings (*27*). Probe diffusion was very sensitive to the casein concentration and PEG size. In addition, we found that the decreases in the diffusion rate of water and small PEGs (620 and 1020 g/mol) followed the same law when the casein concentration increased. Therefore, these small molecules had a similar sensitivity to the presence of micelles. The simplest explanation is that below a certain molecular weight (between 1000 and 8000), PEGs can enter the same space as water with the same facility, and therefore can diffuse through the micelle structure according to the model proposed by Colsenet et al. (*27*). This conclusion is consistent with previous studies, where evidence that large molecules such as $\beta$-casein (24 000 g/mol) (*56, 57*) and transglutaminase (45 000 g/mol) (*58–61*) can enter a casein micelle has been reported. Nevertheless, it is also possible that water and small PEGs follow different pathways but experience a similar obstruction effect.

Despite the different organization of the micelle structure, the diffusion coefficients of molecules with $M_w \leq 1020$ in the gel state were identical after coagulation whatever the gel microstructure (**Figures 11** and **10**). These findings are consistent with those of Mariette et al. (*26*), where water diffusion was reported to be the same in solutions and in the corresponding acid and rennet gels. As we found that small PEGs (620 and 1020 g/mol) and water motion were similarly hindered in solutions by casein micelles, it is not surprising that there was no influence of coagulation on the diffusion of small PEGs. These results demonstrate that modification of the casein network on a microscopic scale has no significant effect on the diffusion of small molecules. For such probes, the main obstruction effect seems to be explained by the proteins themselves and not by the casein aggregate structures.

**Diffusion of Large Molecules.** Above 1020 g/mol, the obstruction mechanism was dependent on the PEG size in casein suspensions (**Figure 6**). As proposed by Colsenet et al. (*27*), this can be explained by considering the balance between the diffusion pathways surrounding and going through the casein micelles. According to this interpretation, larger polymers are more constrained inside a micelle, and hence experience more obstruction effects when diffusing through it. For a given casein concentration of the suspensions, the decrease in the overall diffusion coefficient of a PEG is thus greater for larger polymers.

The casein micelle structure is modified after coagulation because of the internal rearrangements, which result in a matrix structure with more free spaces. According to the SEM images (**Figure 10**) the appearance of the network is highly dependent on the coagulation process. The largest pores were observed for the combined gel, and the smallest were obtained for the acid gel, indicating that fewer rearrangements had taken place. These findings are consistent with previous studies in which gels made by a combination of enzyme action and acidification

were reported to have large pores, highly fused aggregates, high permeability, and unusual rheological properties (*1, 2, 55, 62–64*). According to our NMR data, the increase in the diffusion coefficients after the system coagulation was greater when the casein network appeared more branched, with compact strands and larger pores (**Figures 11** and **10**). Therefore, our results suggest that the diffusion of large PEGs is closely related to the microstructure of the gels and, hence, to the extent of the network rearrangements. These structural changes lead to particle fusions and compactions, resulting in greater permeability where more space is available for molecules to diffuse freely.

It is very interesting to see that, despite significant differences in the coagulation processes and in the final properties of the gels studied, as soon as a network is formed, a common phenomenon can explain the diffusion data. This reasoning is, moreover, very comparable to that proposed by Baldursdottir et al. (*23*) to explain similar results in alginate matrices. The authors reported enhanced PEG diffusion rates in samples that were irradiated, and according to them, the irradiation led to more open networks and thereby facilitated the diffusion of probe molecules. Nevertheless, as illustrated in **Figure 8** for acid gels and previously shown for rennet gels (*27*), these effects were greater for high casein concentrations. This is understandable because, as the casein concentration increases, the casein-free volume decreases in solutions, whereas the empty volume created by the rearrangements is enhanced. In gels, the proportion of the empty volume that results from the gelation process therefore increases with the casein concentration, and hence the effect of coagulation on PEG diffusion is greater when samples are more concentrated.

**Diffusion Behavior of the 527 000 g/mol PEG.** The residues obtained with a biexponential fit (data not shown) revealed that it was not possible to account for only two diffusion coefficients. To correctly describe our data, it was necessary to account for a distribution of diffusion coefficients. In general, such a phenomenon can be caused by several mechanisms that arise from the diffusing molecule itself or from the network. First, the mass polydispersity of the 527 000 g/mol PEG may play a role. Here the polydispersity index of 1.06 given by the manufacturer is consistent with **Figure 4**, and with the $\beta$ value of 0.92 found in a 0.1 M $NaCl/D_2O$ solution (**Figure 5**). However, this mass dispersion cannot explain the observed $\beta$ values of $\sim$0.80, nor its change after coagulation. Other possible explanations for the observed echo decay arise from the presence of heterogeneities inside the matrix (*34*). In our case, the anomalous diffusion behavior of the 527 000 g/mol PEG already appeared in solutions (**Figure 5**) where restricted diffusion, anisotropic diffusion, or large scale heterogeneities should not exist. Casein suspensions are, of course, heterogeneous at the level of casein micelles, but this scale of heterogeneities seems to be too small to explain the curvature observed in the echo decays.

Another important result is that $\beta$ started to decrease in casein suspensions only above a casein concentration of about 9 g/100 g $D_2O$ (**Figure 5**). It was shown for both casein submicelles (*65, 66*) and $\beta$-casein micelle suspensions (*67*) that these spherical particles begin to be close packed at a concentration of approximately 10%. Therefore, the observed decrease in the $\beta$ value might be related to a change in the diffusion regime of the PEG due to the crowding of the system. PEG molecules are known to be highly flexible and can adopt a more linear conformation when the hydrodynamic radius is too large to allow the polymer to diffuse without any constraint on its shape (*68, 69*). Above 9 g/100 g $D_2O$, an elongated shape can thus be expected, and a reptation regime may be assumed. As a result, the length of the PEG might become non-negligible as compared to the distance probed (1.5 $\mu$m), and in that case the PFG-NMR measurements will not record the true center-of-mass motion. The self-diffusion coefficient would thus contain contributions from segmental and rotational mechanisms resulting in non-Fickian behavior. Whatever the underlying causes, a classical echo decay should be recovered when the diffusion interval is sufficiently long, but apparently, this delay can sometimes be too long to be experimentally observed by NMR (*23, 70*).

In the gel state, according to Van Vliet and Walstra (*71*), the casein gels are heterogeneous on several length scales. First, at the scale of the casein particles (as in solutions), heterogeneities are believed to increase in the sense that aggregates are formed and then become more compact with the rearrangements. Second, at the level of the casein strands and nodes, and also at the level of "large aggregates" formed by these strands and nodes, new heterogeneities are formed in the gel state. As observed for the acid gel (**Figure 5**), these heterogeneities should result in a wider distribution of the diffusion coefficients. In contrast, the decrease in the volume of the obstructing elements after coagulation is expected to result in a narrower distribution because the proportion of empty space, and hence the proportion of freely diffusing PEG, increases. Extensive rearrangements inducing larger pores in the gel microstructure should, therefore, not only result in an enhanced mean diffusion rate but also in a decrease in the width of the distribution. This is, in fact, what we observed when comparing the $\beta$ values obtained in the acid, enzymatic, and combined gels (**Figure 5**) with their microstructure (**Figure 10**).

In conclusion, we have shown that, in contrast to small polymers, the diffusion of large PEGs is very sensitive to the microstructure of casein samples. We have also revealed that deviations from a classical diffusion behavior occurred in concentrated solutions and gels for the 527 000 g/mol PEG. The distribution of diffusion coefficients of this large PEG was also found to be affected by the composition and the microstructure of the samples. All these findings could be explained on the basis of network rearrangements that lead to particle fusion and compaction, resulting in a structure where molecules have more free space in which to diffuse. Moreover, depending on the gel formed, the expected extent of structural changes was in very good accordance with the SEM images and literature findings. Probe diffusion has thus proved to be a promising approach for characterizing the structural changes occurring after the establishment of a casein network. Because the PFG-NMR technique is nondestructive and can be repeated over the course of time, further investigations are in progress to reveal whether diffusion experiments could provide dynamic information on these rearrangements.

## ACKNOWLEDGMENT

We thank Mr. Jean-Michel Soulié from SOREDAB for helpful discussions and analyses. We are also grateful to Mr. Armel Guillermo and Mr. Arnaud Bondon for their help with NMR experiments and to Mr. Joseph Le Lannic for assistance with the SEM experiments.

## LITERATURE CITED

(1) Aichinger, P. A.; Michel, M.; Servais, C.; Dillmann, M. L.; Rouvet, M.; D'Amico, N.; Zink, R.; Klostermeyer, H.; Horne, D. S. Fermentation of a skim milk concentrate with *Streptococcus*

*thermophilus* and chymosin: structure, viscoelasticity and syneresis of gels. *Colloids Surf., B* **2003**, *31* (1–4), 243–255.
(2) Lucey, J. A.; Tamehana, M.; Singh, H.; Munro, P. A. Effect of heat treatment on the physical properties of milk gels made with both rennet and acid. *Int. Dairy J.* **2001**, *11* (4–7), 559–565.
(3) Mellema, M.; Heesakkers, J. W. M.; van Opheusden, J. H. J.; van Vliet, T. Structure and scaling behavior of aging rennet-induced casein gels examined by confocal microscopy and permeametry. *Langmuir* **2000**, *16* (17), 6847–6854.
(4) Johansson, L.; Shantze, U.; Lofroth, J. E. Diffusion and interaction in Gels and solutions. 2. Experimental Results on the obstruction effect. *Macromolecules* **1991**, *24* (22), 6019–6023.
(5) Brown, W.; Stilbs, P. Self-diffusion of poly (ethylene oxide) in aqueous dextran solutions measured using FT-pulsed field gradient n.m.r. *Polymer* **1982**, *24*, 188–192.
(6) Masaro, L.; Zhu, X. X.; MacDonald, P. M. Study of the self-diffusion of poly(ethylene glycol)s in poly(vinyl alcohol) aqueous systems. *J. Polymer Sci., B* **1999**, *37* (17), 2396–2403.
(7) Masaro, L.; Zhu, X. X.; Macdonald, P. M. Self-diffusion of oligo- and poly(ethylene glycol)s in poly(vinyl alcohol) aqueous solutions as studied by pulsed-gradient NMR spectroscopy. *Macromolecules* **1998**, *31* (12), 3880–3885.
(8) Nyden, M.; Soderman, O.; Karlstrom, G. A PFG NMR self-diffusion investigation of probe diffusion in an ethyl(hydroxyethyl)cellulose matrix. *Macromolecules* **1999**, *32* (1), 127–135.
(9) Walderhaug, H.; Nystrom, B. A pulsed field gradient NMR study of poly(oxyethylene) diffusion in aqueous solutions and gels of ethyl (hydroxyethyl) cellulose-sodium dodecyl sulphate systems. *Colloids Surf., A* **1999**, *149* (1–3), 379–387.
(10) Jo, B. W.; Hess, M.; Zahres, M. Self-diffusion of poly (ethylene oxide) − modified paclitaxel in dilute aqueous solutions. *Mater, Res. Innovations* **2003**, *7* (3), 178–182.
(11) Petit, J. M.; Zhu, X. X.; Macdonald, P. M. Solute probe diffusion in aqueous solutions of poly(vinyl alcohol) as studied by pulsed-gradient spin-echo NMR spectroscopy. *Macromolecules* **1996**, *29* (1), 70–76.
(12) Griffiths, P. C.; Stilbs, P.; Yu, G. E.; Booth, C. Role of Molecular Architecture in Polymer Diffusion − a PGSE-NMR Study of Linear and Cyclic Poly(Ethylene Oxide). *J. Phys. Chem.* **1995**, *99* (45), 16752–16756.
(13) Hakansson, B.; Nyden, M.; Söderman, O. The influence of polymer molecular-weight distributions on pulsed field gradient nuclear magnetic resonance self-diffusion experiments. *Colloid Polym. Sci.* **2000**, *278* (5), 399–405.
(14) Masaro, L.; Ousalem, M.; Baille, W. E.; Lessard, D.; Zhu, X. X. Self-diffusion studies of water and poly (ethylene glycol) in solutions and gels of selected hydrophilic polymers. *Macromolecules* **1999**, *32* (13), 4375–4382.
(15) Matsukawa, S.; Ando, I. A study of self-diffusion of molecules in polymer gel by pulsed-gradient spin-echo $^1$H NMR. *Macromolecules* **1996**, *29*, 7136–7140.
(16) Matsukawa, S.; Ando, I. Study of self-diffusion of molecules in a polymer gel by pulsed-gradient spin-echo $^1$H-NMR. 2: Intermolecular hydrogen-bond interaction between the proble polymer and network polymer in N,N-dimethylacrylamide-acrylic acid copolymers gel systems. *Macromolecules* **1997**, *30* (26), 8310–8313.
(17) Kwak, S.; Lafleur, M. Self-diffusion of macromolecules and macroassemblies in Curdlan gels as examined by PFG-SE NMR technique. *Colloids Surf., A* **2003**, *221* (1–3), 231–242.
(18) Colsenet, R.; Soderman, O.; Mariette, F. Effects of ionic strength and denaturation time on polyethyleneglycol self-diffusion in whey protein solutions and gels visualized by nuclear magnetic resonance. *J. Agric. Food Chem.* **2006**, *54* (14), 5105–5112.
(19) Trampel, R.; Schiller, J.; Naji, L.; Stallmach, F.; Kärger, J.; Arnold, K. Self-diffusion of polymers in cartilage as studied by pulsed field gradient NMR. *Biophys. Chem.* **2002**, *97* (2–3), 251–260.
(20) Newling, B. Pulsed Field Gradient NMR Study of the Diffusion of $H_2O$ and Polyethylene Glycol Polymers in the Supramolecular Structure of Wet Cotton. *J. Phys. Chem. B* **2003**, *107*, 12391–12397.
(21) Weng, L. H.; Liang, S. M.; Zhang, L.; Zhang, X. M.; Xu, J. Transport of glucose and poly(ethylene glycol)s in agarose gels studied by the refractive index method. *Macromolecules* **2005**, *38* (12), 5236–5242.
(22) Favre, E.; Leonard, M.; Laurent, A.; Dellacherie, E. Diffusion of polyethyleneglycols in calcium alginate hydrogels. *Colloids Surf., A* **2001**, *194* (1–3), 197–206.
(23) Baldursdottir, S. G.; Kjoniksen, A.-L.; Nystrom, B. The effect of riboflavin-photoinduced degradation of alginate matrices on the diffusion of poly(oxyethylene) probes in the polymer network. *Eur. Polym. J.* **2006**, *42* (11), 3050–3058.
(24) Metais, A.; Cambert, M.; Riaublanc, A.; Mariette, F. Influence of fat globule membrane composition on water holding capacity and water mobility in casein rennet gel: A nuclear magnetic resonance self-diffusion and relaxation study. *Int. Dairy J.* **2006**, *16* (4), 344–353.
(25) Métais, A.; Cambert, M.; Riaublanc, A.; Mariette, F. Effects of casein and fat content on water self-diffusion coefficients in casein systems: a pulsed field gradient nuclear magnetic resonance study. *J. Agric. Food Chem.* **2004**, *52* (12), 3988–3995.
(26) Mariette, F.; Topgaard, D.; Jönsson, B.; Söderman, O. $^1$H NMR diffusometry study of water in casein dispersion and gels. *J. Agric. Food Chem.* **2002**, *50* (15), 4295–4302.
(27) Colsenet, R.; Soderman, O.; Mariette, F. Effect of casein concentration in suspensions and gels on poly(ethylene glycol)s NMR self-diffusion measurements. *Macromolecules* **2005**, *38* (22), 9171–9179.
(28) Glasoe, P. K.; Long, F. A. Use of glass electrodes to measure acidities in deuterium oxide. *J. Phys. Chem.* **1960**, *64* (1), 188–190.
(29) Wu, D. H.; Chen, A. D.; Johnson, C. S. An Improved Diffusion-Ordered Spectroscopy Experiment Incorporating Bipolar-Gradient Pulses. *J. Magn. Reson. Ser. A* **1995**, *115* (2), 260–264.
(30) Gibbs, S. J. Observations of Diffusive Diffraction in a Cylindrical Pore by PFG NMR. *J. Magn. Reson.* **1997**, *124* (1), 223–226.
(31) Johnson, C. S. Diffusion ordered nuclear magnetic resonance spectroscopy: principles and applications. *Prog. Nucl. Magn. Reson. Spectrosc.* **1999**, *34* (3–4), 203–256.
(32) Nystrom, B.; Walderhaug, H.; Hansen, F. K. Dynamic Crossover Effects Observed in Solutions of a Hydrophobically Associating Water-Soluble Polymer. *J. Phys. Chem.* **1993**, *97* (29), 7743–7752.
(33) Abrahmsenalami, S.; Stilbs, P. $^1$H-NMR Self-Diffusion and Multifield $^2$H Spin Relaxation Study of Model Associative Polymer and Sodium Dodecyl-Sulfate Aggregation in Aqueous-Solution. *J. Phys. Chem.* **1994**, *98* (25), 6359–6367.
(34) Nyden, M.; Soderman, O. An NMR self-diffusion investigation of aggregation phenomena in solutions of ethyl(hydroxyethyl) cellulose. *Macromolecules* **1998**, *31* (15), 4990–5002.
(35) Walderhaug, H.; Nyström, B. Anomalous diffusion in an aqueous system of a poly (ethylene oxide) - poly (propylene oxide) triblock copolymer during gelation studied by pulsed field gradient NMR. *J. Phys. Chem.* **1997**, *101*, 1524–1528.
(36) Shapiro, Y. E. Compartmentation in the poly(vinyl alcohol) cryogels. $^1$H NMR self-diffusion study. *Colloids Surf., A* **2000**, *164* (1), 71–83.
(37) McMahon, D. J.; Brown, R. J. Composition, Structure, and Integrity of casein micelles: a review. *J. Dairy Sci.* **1984**, *67*, 499–512.
(38) Horne, D. S. Casein interactions: Casting light on the black boxes, the structure in dairy products. *Int. Dairy J.* **1998**, *8* (3), 171–177.
(39) Marchin, S.; Putaux, J. L.; Pignon, F.; Leonil, J. Effects of the environmental factors on the casein micelle structure studied by cryo transmission electron microscopy and small-angle x-ray scattering/ultrasmall-angle x-ray scattering. *J. Chem. Phys.* **2007**, *126*, (4).
(40) Lucey, J. A. Formation and physical properties of milk protein gels. *J. Dairy Sci.* **2002**, *85* (2), 281–294.

(41) Horne, D. S. Casein micelles as hard spheres: limitations of the model in acidified gel formation. *Colloids Surf., A* **2003**, *213* (2–3), 255–263.

(42) Walstra, P. On the stability of casein micelles. *J. Dairy Sci.* **1990**, *73*, 1968–1979.

(43) Holt, C.; Horne, D. S. The hairy casein micelle: Evolution of the concept and its implications for dairy technology. *Neth. Milk Dairy J.* **1996**, *50* (2), 85–111.

(44) Kumosinski, T. F.; Pessen, H.; Farrell, H. M.2, Jr.; Brumberger, H. Determination of the quaternary structural states of bovine casein by small-angle X-Ray scattering: submicellar and micellar forms. *Arch. Biochem. Biophys.* **1988**, *266*, 548–561.

(45) Guillaume, C.; Jimenez, L.; Cuq, J. L.; Marchesseau, S. An original pH-reversible treatment of milk to improve rennet gelation. *Int. Dairy J.* **2004**, *14* (4), 305–311.

(46) Gastaldi, E.; Lagaude, A.; Marchesseau, S.; DelaFuente, B. T. Acid milk gel formation as affected by total solids content. *J. Food Sci.* **1997**, *62* (4), 671.

(47) Vetier, N.; Banon, S.; Ramet, J. P.; Hardy, J. Casein micelle solvation and fractal structure of milk aggregates and gels. *Lait* **2000**, *80* (2), 237–246.

(48) Karlsson, A. O.; Ipsen, R.; Schrader, K.; Ardo, Y. Relationship between physical properties of casein micelles and rheology of skim milk concentrate. *J. Dairy Sci.* **2005**, *88* (11), 3784–3797.

(49) Mellema, M.; Walstra, P.; Van Opheusden, J. H. J.; Van Vliet, T. Effects of structural rearrangements on the rheology of rennet-induced casein particle gels. *Adv. Colloid Interface Sci.* **2002**, *98* (1), 25–50.

(50) Lucey, J. A.; van Vliet, T.; Grolle, K.; Geurts, T.; Walstra, P. Properties of acid casein gels made by acidification with gluconо-$\delta$-lactone. 2. Syneresis, permeability and microstructural properties. *Int. Dairy J.* **1997**, *7* (6–7), 389–397.

(51) Bauer, R.; Hansen, M.; Hansen, S.; Ogendal, L.; Lomholt, S.; Qvist, K.; Harne, D. The Structure of Casein Aggregates During Renneting Studied by Indirect Fourier Transformation and Inverse Laplace Transformation of Static and Dynamic Light-Scattering Data, Respectively. *J. Chem. Phys.* **1995**, *103* (7), 2725–2737.

(52) Lagoueyte, N.; Lablee, J.; Lagaude, A.; Delafuente, B. T. Temperature affects microstructure of renneted milk gel. *J. Food Sci.* **1994**, *59* (5), 956–959.

(53) Lucey, J. A.; van Vliet, T.; Grolle, K.; Geurts, T.; Walstra, P. Properties of acid casein gels made by acidification with gluconо-$\delta$-lactone. 1. Rheological properties. *I. Dairy J.* **1997**, *7* (6–7), 381–388.

(54) Lucey, J. A.; Tamehana, M.; Singh, H.; Munro, P. A. A comparison of the formation, rheological properties and microstructure of acid skim milk gels made with a bacterial culture or glucono-delta-lactone. *Food Res. Int.* **1998**, *31* (2), 147–155.

(55) Van Vliet, T.; Lakemond, C. M. M.; Visschers, R. W. Rheology and structure of milk protein gels. *Curr. Opin. Colloid Interface Sci.* **2004**, *9* (5), 298–304.

(56) Creamer, K.; Berry, G. P.; Mills, O. E. A study of the dissociation of $\beta$-casein of the bovin casein micelle at low temperature. *N. Z. J. Dairy Sci. Technol.* **1997**, *12*, 58.

(57) Dalgeish, D. G.; Law, J. R. pH-induced dissociation of bovine casein micelles. 2. mineral solubilization and its relation to casein release. *J.Dairy Res.* **1989**, *56*, 727–735.

(58) De Kruif, C. G.; Tuinier, R.; Holt, C.; Timmins, P. A.; Rollema, H. S. Physicochemical study of $\kappa$- and $\beta$-casein dispersions and the effect of cross-linking by transglutaminase. *Langmuir* **2002**, *18* (12), 4885–4891.

(59) O'Connell, J. E.; De Kruif, C. G. $\beta$-casein micelles; cross-linking with transglutaminase. *Colloids Surf., A* **2003**, *216* (1–3), 75–81.

(60) Schorsch, C.; Carrie, H.; Clark, A. H.; Norton, I. T. Cross-linking casein micelles by a microbial transglutaminase conditions for formation of transglutaminase-induced gels. *Int. Dairy J.* **2000**, *10* (8), 519–528.

(61) Schorsch, C.; Carrie, H.; Norton, I. T. Cross-linking casein micelles by a microbial transglutaminase: influence of cross-links in acid-induced gelation. *Int. Dairy J.* **2000**, *10* (8), 529–539.

(62) Lucey, J. A.; Tamehana, M.; Singh, H.; Munro, P. A. Rheological properties of milk gels formed by a combination of rennet and glucono-$\delta$-lactone. *J. Dairy Res.* **2000**, *67* (3), 415–427.

(63) Tranchant, C. C.; Dalgleish, D. G.; Hill, A. R. Different coagulation behaviour of bacteriologically acidified and renneted milk: the importance of fine-tuning acid production and rennet action. *Int. Dairy J.* **2001**, *11* (4–7), 483–494.

(64) Lopez, M. B.; Lomholt, S. B.; Qvist, K. B. Rheological properties and cutting time of rennet gels. Effect of pH and enzyme concentration. *Int. Dairy J.* **1998**, *8* (4), 289–293.

(65) Farrer, D.; Lips, A. On the self-assembly of sodium caseinate. *Int. Dairy J.* **1999**, *9*, 281–286.

(66) Panouille, M.; Benyahia, L.; Durand, D.; Nicolai, T. Dynamic mechanical properties of suspensions of micellar casein particles. *J. Colloid Interface Sci.* **2005**, *287* (2), 468–475.

(67) Panouille, M.; Durand, D.; Nicolai, T. Jamming and gelation of dense $\beta$-casein micelle suspensions. *Biomacromolecules* **2005**, *6* (6), 3107–3111.

(68) De Gennes, P. G. Reptation of a polymer chanin in the presence of fixed obstacles. *J. Chem. Phys.* **1971**, *55* (2), 572–579.

(69) De Gennes, P. G. Brownian motions of flexible poymer chains. *Nature* **1979**, *282*, 367–370.

(70) Rosen, O.; Bostrom, M.; Nyden, M.; Piculell, L. Anomalous surfactant diffusion in a gel of chemically cross-linked ethyl(hydroxyethyl) cellulose. *J. Phys. Chem. B* **2003**, *107* (17), 4074–4079.

(71) Van Vliet, T.; Walstra, P. Water in Casein Gels - How to Get It Out or Keep It in. *J. Food Eng.* **1994**, *22* (1–4), 75–88.

**Received for review July 3, 2007. Revised manuscript received October 8, 2007. Accepted October 18, 2007. The authors thank the Regional Council of Brittany and SOREDAB for financial support.**

JF071982V